JOURNAL OF GEOPHYSICAL RESEARCH, VOL. 91, NO. D1, PAGES 1137–1152, JANUARY 20, 1986

Concentrations and Uncertainties of Stratospheric Trace Species Inferred From Limb Infrared Monitor of the Stratosphere Data 2. Monthly Averaged OH, HO_2, H_2O_2, and HO_2NO_2

JACK A. KAYE AND CHARLES H. JACKMAN

Atmospheric Chemistry and Dynamics Branch, NASA Goddard Space Flight Center Greenbelt, Maryland

Monthly, zonally averaged limb infrared monitor of the stratosphere data from the Nimbus 7 satellite are used with an essentially algebraic photochemical equilibrium model presented in part 1 of this series (Kaye and Jackman, this issue) to infer concentrations and uncertainties of the odd hydrogen species OH, HO_2, H_2O_2, and HO_2NO_2 as a function of altitude, latitude, and season. The inferred concentrations for OH and H_2O_2 are found to be reasonably consistent with some but not all previous observations; most of the inferred HO_2 concentrations are below those which have been observed. Concentrations of all inferred species at mid-latitudes are expected to maximize in the summer. Uncertainties u_i are found to be largest in the lower stratosphere for all species and to decrease approximately in the order $u_{H_2O_2} > u_{HO_2NO_2} > u_{HO_2} > u_{OH}$ over most of the stratosphere. In the tropics and at mid-latitudes the variation of the uncertainties with latitude and season is substantially smaller than the inferred variation of the concentrations.

1. Introduction

One of the major results to come from studies of stratospheric chemistry in recent years is the crucial role which short-lived intermediate (transient) species, present in very small trace amounts (<10 ppbv), can play in controlling the concentration of longer lived and more prevalent species, especially ozone (O_3) [World Meteorological Organization (WMO), 1982]. In particular, attention has focused on the free radical species OH, HO_2, ClO, NO, and NO_2. These species can lead to alterations, primarily reductions, in O_3 concentrations through cyclic processes [*Johnston and Podolske*, 1978; *DeMore and Yung*, 1982] in which the free radical species catalytically converts O_3 or O to O_2 by reactions which are significantly faster than the Chapman reactions:

$$O + O_3 \rightarrow 2O_2$$

$$O + O + M \rightarrow O_2 + M$$

Thus detailed knowledge of the concentrations of transient free radicals in the stratosphere is important, especially for the accurate assessment of possible long-term reductions in stratospheric ozone by the increased concentration of odd chlorine (Cl, ClO, HCl, HOCl, $ClNO_3$) and odd nitrogen (NO, NO_2, HNO_3, HO_2NO_2, NO_3, N_2O_5) derived from anthropogenic sources [*National Academy of Sciences* (NAS), 1984]. At present, however, there exist only very limited observational data on the concentrations of stratospheric free radicals. What data do exist are relatively sparse; for no transient species other than NO_2 are there data for a variety of latitudes, seasons, altitudes, and times of day, all of which are necessary for the verification of multidimensional models of stratospheric chemistry and dynamics under development. Without the existence of a large data base, it is also difficult to know what portion of disagreement between observations and model predictions is due to atmospheric variability or to either observational errors or errors in the input and/or formulation of the models.

Paper number 5D0703.

For some time, it has been recognized that the daytime concentrations of some trace species could in principle be inferred from those of longer-lived or more prevalent species by assumption of photochemical equilibrium, which is, in general, a quite accurate one through much of the stratosphere for many species. For example, a simple relationship between the OH concentration and the ratio of NO_2 and HNO_3 concentration has been known for some time [*Evans et al.*, 1976; *Harries*, 1978]. *Harries* [1982] demonstrated how one might infer the concentration of ClO from the observed concentrations of several other species. In a slightly different approach, *Allam et al.* [1981] inferred global distributions of OH from those of O_3 and H_2O calculated in a stratospheric general circulation model.

The recent availability of constituent fields from satellite-based experiments has given impetus to the attempt to infer concentrations of transient species from those of longer-lived, more easily observed molecules. These experiments are the limb infrared monitor of the stratosphere (LIMS) [*Gille and Russell*, 1984] and stratospheric and mesospheric sounder (SAMS) [*Rodgers et al.*, 1984], and solar backscattered ultraviolet instrument (SBUV) [*McPeters et al.*, 1984] on the Nimbus 7 satellite, and the Solar Mesosphere Explorer (SME) satellite [*Barth et al.*, 1983]. The measurements include O_3 [*Remsberg et al.*, 1984*a*], H_2O [*Russell et al.*, 1984*a*; *Remsberg et al.*, 1984*b*], HNO_3 [*Russell et al.*, 1983; *Gille et al.*, 1984*a*] NO_2 [*Russell et al.*, 1984*b*, *c*], and temperature [*Gille et al.*, 1984*b*] from LIMS, CH_4 and N_2O from SAMS [*Jones and Pyle*, 1984; *Jones*, 1984], O_3 from SBUV [*McPeters et al.*, 1984], and O_3 and NO_2 in the upper stratosphere (and mesosphere) from SME [*Mount et al.*, 1983, 1984; *Thomas et al.*, 1984].

These data, especially the LIMS data, have been used in attempts to infer concentration of transient species. *Pyle et al.* [1983, 1984] used the LIMS daytime HNO_3 and NO_2 measurements to infer daytime concentrations of OH over most of the stratosphere by the ratio method suggested earlier [*Evans et al.*, 1976; *Harries*, 1978]. This method was also demonstrated by *Gille et al.* [1984*a*] in their LIMS HNO_3 validation paper. *Jackman et al.* [1985*a*] demonstrated that this method must be applied cautiously, since if the LIMS

data are used without correction, unphysically large or negative OH concentrations were obtained above 5 mbar. They then showed an alternative way for inferring stratospheric OH from LIMS data using a method in which photochemical equilibrium for total odd hydrogen ($=OH + H + HO_2 + HNO_3 + HO_2NO_2 + 2H_2O_2$) is assumed. They also used this inferred OH distribution and the other LIMS measurements to compute a revised HNO_3 profile which is more reasonable than the LIMS observed profile above 5 mbar.

Most recently, we [*Kaye and Jackman*, this issue] (hereafter referred to as KJ) used LIMS and SAMS data together with an essentially algebraic model for stratospheric photochemistry to derive concentrations and uncertainties of a variety of HO_x and NO_x species. Similarly, Pyle and coworkers [*Pyle et al.*, 1984; *Pyle and Zavody*, 1985] derived concentrations of stratospheric OH, HO_2, and H_2O_2, along with uncertainties for OH (the latter were obtained by numerically varying initial concentrations, reaction rates, and photolysis rates within their stated uncertainties).

In this work, we extend our previous work (KJ) to calculate monthly zonal averages of concentrations and uncertainties for the HO_x species OH, HO_2, H_2O_2, and HO_2NO_2. OH and HO_2 are important because they are the major odd hydrogen free radical species in the upper and lower stratosphere, respectively. They play a crucial role in the partitioning of NO_x and ClO_x species among their various members and are thus of great interest [see *WMO*, 1982].

H_2O_2 is a potentially important odd hydrogen reservoir species, although published observations indicate that it is present in amounts not much more than (and possibly considerably less than) 1 ppbv [*Waters et al.*, 1981; *Chance and Traub*, 1984]. It is expected to have a great deal of variability [*Connell et al.*, 1985], so knowledge of a monthly zonal average could be important in comparing observations and models. It has been suggested [*Derwent and Eggleton*, 1981] that its measurement, combined with other species, could lead to the ability to discriminate among various one-dimensional models.

HO_2NO_2 is now thought to be an important species in controlling odd hydrogen concentrations in the lower stratosphere [*WMO*, 1982], but the only measurement reported [*NASA*, 1979] is one of Murcray and coworkers, who estimate an upper limit of 0.4 ppbv. Thus knowledge of monthly zonal averages may be of use in planning future measurements.

We compare our inferred concentrations to two-dimensional stratospheric models and, where available, remote and in situ observations. We consider especially the magnitude of the inferred monthly variability in concentration as a function of latitude and altitude. We also examine the monthly variability in the total uncertainties, as well as the relative magnitude of the monthly variability and the total uncertainty.

The outline of this paper is as follows. In section 2 we briefly review the method of inferring the concentrations and uncertainties of the species under study. In section 3 we present our results, mainly in the form of figures. In section 4 we discuss the results, including a comparison with model and observational results. Finally, in section 5 we summarize the results obtained and restate the conclusions of this study.

2. Method and Calculations

The algebraic model used and the model input parameters have been discussed extensively in our previous paper (KJ), so we will only briefly summarize them here. Daytime trace species concentrations are inferred from the daytime LIMS measurements of O_3 [*Remsberg et al.*, 1984*a*], H_2O [*Russell et al.*, 1984*b*,], HNO_3 [*Gille et al.*, 1984*a*], NO_2 [*Russell et al.*, 1984*b*, *c*], and temperature [*Gille et al.*, 1984*b*], the SAMS CH_4 zonal monthly averages, where available [*Jones and Pyle*, 1984], and model profiles for CO, H_2, and CH_4 (where SAMS data were not available) derived from the Goddard two-dimensional diabatic circulation model [*Guthrie et al.*, 1984*b*]. Chemical reaction rates and absorption cross sections used are from the sixth Jet Propulsion Laboratory (JPL) memorandum [*DeMore et al.*, 1983]. Uncertainties in input concentrations come from the appropriate validation papers, while those of reaction rates (corresponding to one standard deviation) and photolysis rates are from *DeMore et al.* [1983]. Uncertainties in model-derived profiles were arbitrarily picked but, as explained previously (KJ), are not crucial for most of the species considered here.

HO_x species concentrations are obtained by assuming total odd hydrogen to be in photochemical equilibrium

$$P(\text{Total Odd Hydrogen}) = L(\text{Total Odd Hydrogen}) \quad (1)$$

where P stands for production, L stands for loss, the total odd hydrogen is given approximately by the relationship

$$\begin{aligned}\text{Total Odd Hydrogen} = {} & [OH] + [H] + [HO_2] \\ & + [HNO_3] + [HO_2NO_2] \\ & + 2[H_2O_2] + [CH_3O] + [CH_3O_2] \\ & + [CH_3] + [HCO] \quad (2)\end{aligned}$$

The terms in (1) are given in equation (13) of our earlier work (KJ). The most important terms in the odd hydrogen production is the production of OH by reaction of $O(^1D)$ (produced by photolysis of O_3) with H_2O:

$$O(^1D) + H_2O \rightarrow 2OH \quad (3)$$

In the lower stratosphere, hydrocarbon oxidation and loss terms are also important, primarily by

$$O(^1D) + CH_4 \rightarrow OH + CH_3 \quad (4)$$

$$CH_2O + h\nu \rightarrow H + HCO \quad (5)$$

Other terms (i.e., H_2O photolysis, reaction of $O(^1D)$ with H_2, etc.) are fairly small.

Odd hydrogen loss is, to a very good approximation, due to three reactions:

$$OH + HO_2 \rightarrow H_2O + O_2 \quad (6)$$

$$OH + HNO_3 \rightarrow H_2O + NO_3 \quad (7)$$

$$OH + HO_2NO_2 \rightarrow H_2O + NO_2 + O_2 \quad (8)$$

The concentrations of HO_2, HO_2NO_2, and CH_2O are obtained with the assumption of photochemical equilibrium. The major processes involved in OH-HO_2 interconversion are

$$OH + O_3 \rightarrow HO_2 + O_2 \quad (9)$$

$$HO_2 + NO \rightarrow OH + NO_2 \quad (10)$$

$$HO_2 + O_3 \rightarrow OH + 2O_2 \quad (11)$$

$$HO_2 + O \rightarrow OH + O_2 \quad (12)$$

If the lower stratosphere one must also consider the reaction

$$CO + OH \rightarrow CO_2 + H \quad (13)$$

followed by the reaction

$$H + O_2 + M \rightarrow HO_2 + M \quad (14)$$

while in the upper stratosphere one must include

$$O + OH \rightarrow O_2 + H \quad (15)$$

which is followed either by reaction (14) or by

$$H + O_3 \rightarrow OH + O_2 \quad (16)$$

HO_2NO_2 is calculated assuming that only the following processes are involved in its production and destruction:

$$HO_2 + NO_2 + M \rightarrow HO_2NO_2 + M \quad (17)$$

$$HO_2NO_2 + h\nu \rightarrow HO_2 + NO_2 \quad (18a)$$

$$HO_2NO_2 + h\nu \rightarrow OH + NO_3 \quad (18b)$$

and equation (8):

$$OH + HO_2NO_2 \rightarrow H_2O + NO_2 + O_2$$

For reactions involving CH_2O, which will not be explicitly considered here, the reader is referred to our earlier paper (KJ). As discussed in the earlier work, the coupled photochemical equations may not be solved analytically, but are, instead, iterated to achieve a solution.

One major assumption in our photochemical model is the neglect of odd chlorine (Cl_x) species. The reason for and validity of this neglect has been discussed in great detail in our previous paper (KJ), and we only briefly summarize here our reasons for expecting this assumption to be valid. Cl_x is only expected to have an effect on the patitioning of odd hydrogen compounds (especially, OH and HO_2) and not on the total amount of odd hydrogen. This occurs because the odd hydrogen production reactions (3)–(5) are much faster than the Cl_x-induced odd hydrogen production reaction

$$Cl + CH_4 \rightarrow HCl + CH_3$$

while the odd hydrogen destruction reactions (6)–(8) are also much faster than the corresponding Cl_x-induced one

$$OH + HCl \rightarrow H_2O + Cl$$

We showed previously (KJ) that at mid-latitudes each of these made up less than 10% of the corresponding total rate and the combined contribution should be smaller.

Cl_x could affect the partitioning of OH and HO_2 mainly by affecting the partitioning of odd nitrogen between NO and NO_2 because of the important role of NO in HO_2 to OH interconversion (reaction (10)). Neglect of ClO could lead to an overestimate of the correct NO concentration by an amount up to 25% at 40 km at mid-latitudes. However, at such high altitudes, HO_2-OH interconversion is dominated by reaction with atomic oxygen (reaction (12)), so that this overestimate of NO should contribute no more than 10% to the HO_2 and OH concentrations. Lower in the stratosphere, where reaction (10) dominates HO_2-OH interconversion, ClO is small, and the error in the NO concentration is smaller, so that the net error in the OH and HO_2 concentrations is also small.

Total uncertainties are calculated using the estimated model input uncertainties f_j and the sensitivity coefficients S_{ij}

$$S_{ij} = \partial \ln [M_i] / \partial \ln P_j \quad (19)$$

where $[M_i]$ is the inferred concentration of species i and P_j is some model input parameter (concentration, reaction rate, photolysis rate). Each S_{ij} is obtained by solving directly (or iterating) the partial derivative of the appropriate equation in the algebraic model. Individual parameter uncertainties, the sources of which have been described above and which have been presented in detail in our earlier work (KJ) and the corresponding sensitivity coefficients are used to calculate the total uncertainty u_i in parameter i by

$$u_i = \exp \left[\sum_j (S_{ij} \ln f_j)^2 \right]^{1/2} \quad (20)$$

Equation (20) has been used for atmospheric chemistry in a somewhat different sense by previous workers [*NAS*, 1976; *Butler*, 1978, 1979; *Stolarski*, 1980].

Photolysis rates were calculated using the radiation package of the Goddard two-dimensional model [*Guthrie et al.*, 1984*a*] modified to include the effects of multiple scattering [*Jackman et al.*, 1985*a*, *b*] assuming a local time of noon. Since the LIMS satellite did not obtain data at precisely noon local time (deviations are of the order of 1 hour in the tropics and mid-latitudes and become larger near the limits of the data field at 64°S and 84°N), one should treat the results closest to the poles with some care. At these latitudes the photochemical equilibrium approximation will begin to break down for many species, altitudes, and seasons, and it was thus felt that many of the high-latitude results would be at most qualitatively correct, anyway. This effect should be most severe south of 50°S in southern hemisphere fall and spring, where one is fairly close to the terminator, and a few hours change in local time can cause conditions to change from maximum daylight to total darkness. In the northern polar region, where deviations from noon in local time of the satellite measurements are smaller, this constraint is somewhat less severe, although it should still be considered in interpreting our results.

Monthly, zonal averages of daytime LIMS data (solar zenith angle $<90°$) were obtained from the LIMS profile tapes from the National Space Sciences Data Center (NSSDC) at the Goddard Space Flight Center. Quantities were zonally averaged and binned according to the two-dimensional grid used by *Guthrie et al.* [1984*a*, *b*] in their diabatic circulation model.

3. Results

The results of this study consist of concentrations and uncertainties of OH, HO_2, H_2O_2, and HO_2NO_2 as a function of latitude and altitude for each of the seven months (November–May) for which LIMS data are available. With the two-dimensional grid we used, this corresponds to some 7500 different concentrations and an equal number of uncertainties. Sensitivity coefficients of the output species with respect to all the model input parameters were also calculated, which would lead to a factor of 10 more data. Because of this large amount of data we will consider here only a limited subset of the concentration and uncertainty data and will consider the sensitivity coefficients only briefly in the discussion section. We will focus our attention on the magnitude of the various quantities and their variation with latitude, altitude, and season, paying special attention to the 35°N latitude region, as that is close to the latitude of Palestine, Texas, the site of many balloon launches and a representative mid-latitude area. We will also consider one representative tropical latitude (5°N) and one near-polar (65°N) latitude.

Contour diagrams showing zonal monthly averaged mixing ratios of OH, HO_2, H_2O_2, and HO_2NO_2 are shown in Figure 1 for the months of December and March. Considering both

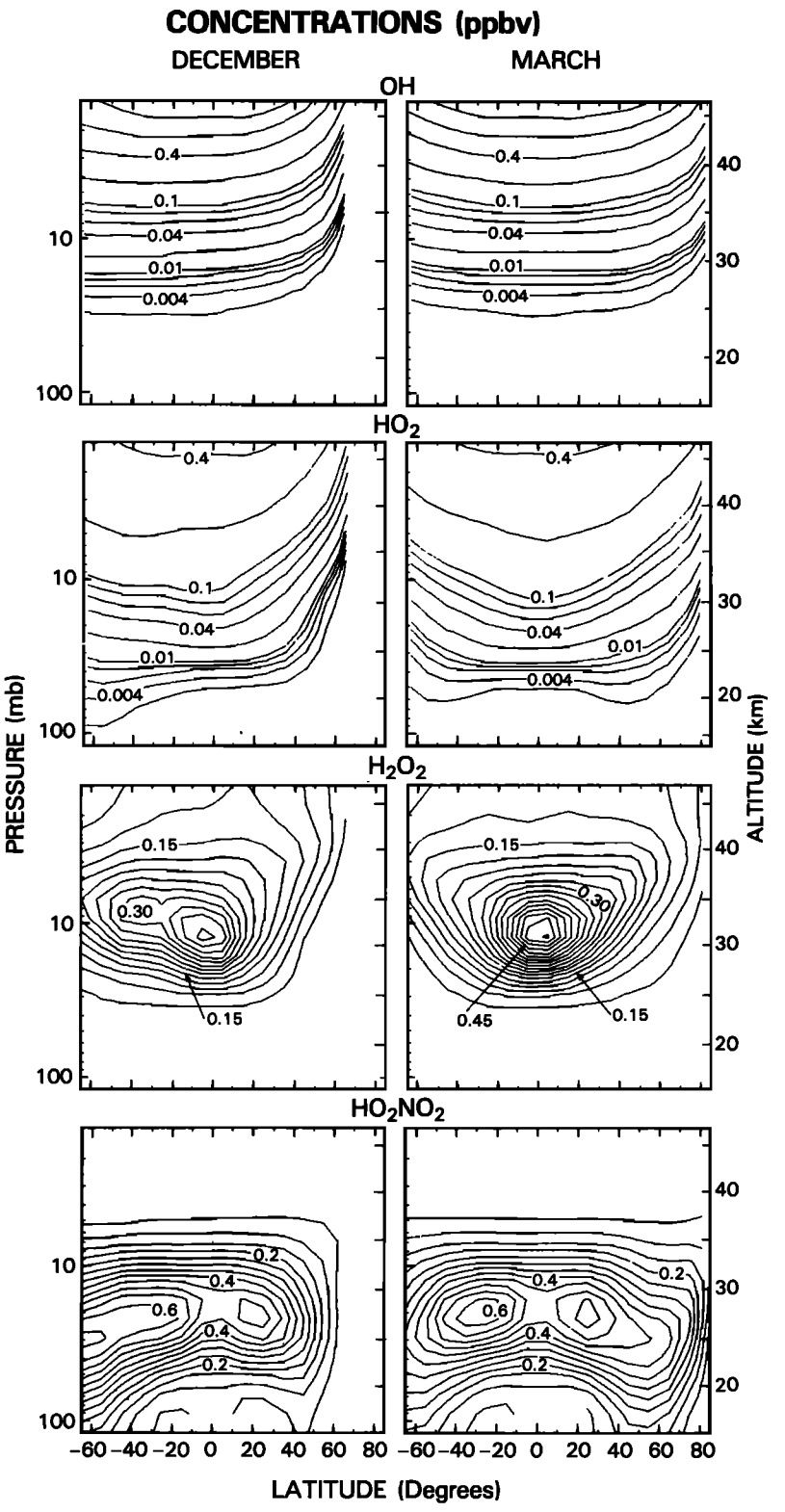

Fig. 1. Contour plots showing latitude-altitude calculated distribution of daytime OH (top row), HO_2 (second row), H_2O_2 (third row), and HO_2NO_2 (fourth row) mixing ratios plotted in ppbv for the months of December (left column) and March (right column). No data are plotted for December above 65°N because this corresponds to the polar night region. Contours for OH and HO_2 are drawn at values $A \times 10^E$ ppbv where $A = 2, 4, 6, 8, 10$ and $E = -3, -2, -1$. Contours for H_2O_2 and HO_2NO_2 are drawn every 0.03 and 0.05 ppbv, respectively.

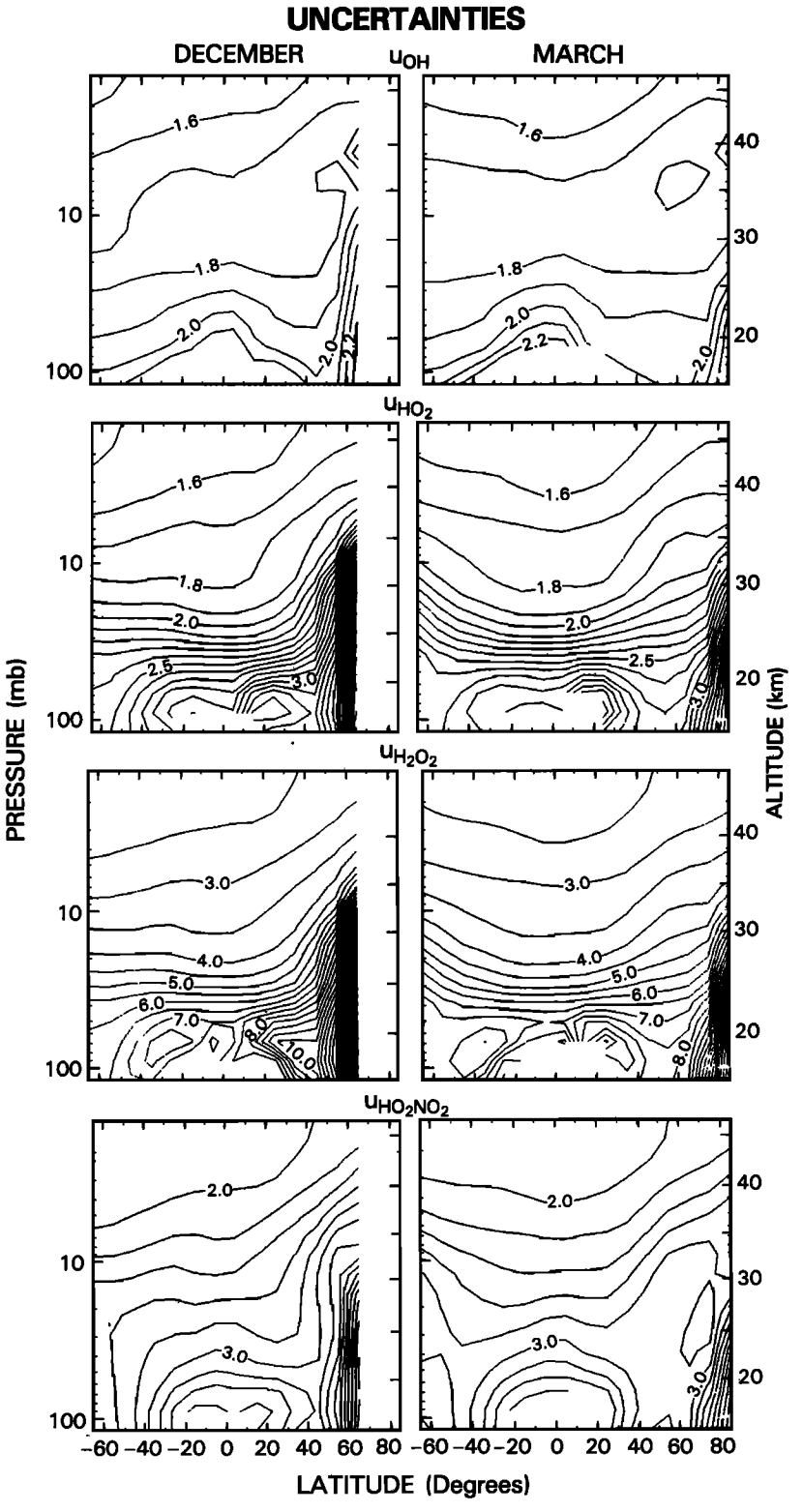

Fig. 2. Contour plots showing calculated uncertainties in inferred OH, HO_2, H_2O_2, and HO_2NO_2 concentrations. Plots are arranged as are those of concentration in Figure 1. Contour intervals are 0.1 for OH and HO_2, 0.5 for H_2O_2, and 0.2 for HO_2NO_2.

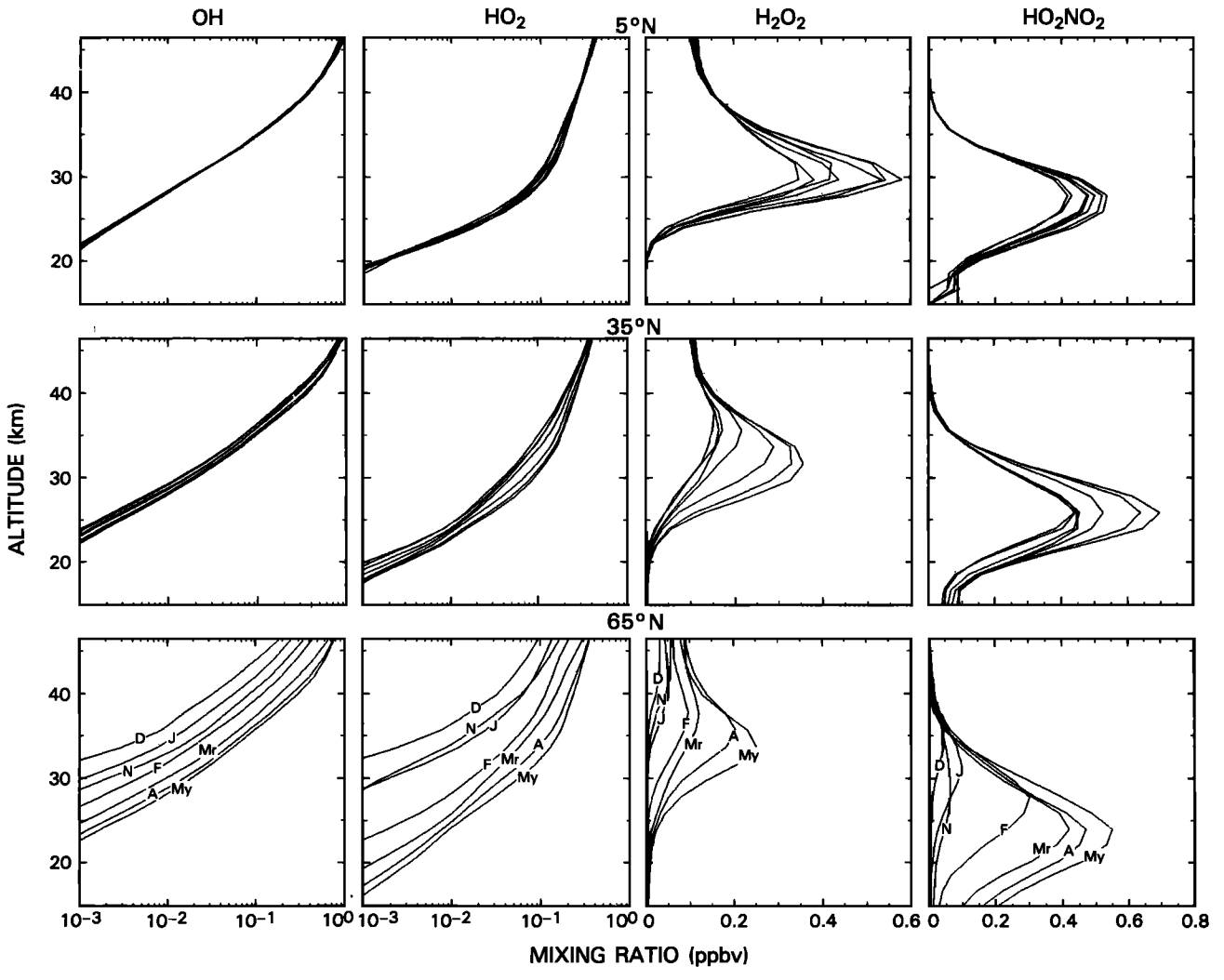

Fig. 3. Altitude-mixing ratio plots for inferred amounts of OH (first column), HO_2 (second column), H_2O_2 (third column), and HO_2NO_2 (fourth column) for the latitudes 5°N (top row), 35°N (middle row), and 65°N (bottom row). Individual curves are labeled only for 65°N. Letters represent first letters of corresponding months. March and May are designated as Mr and My, respectively.

hemispheres, these 2 months cover all four seasons (northern hemisphere winter and spring, southern hemisphere fall and summer). The corresponding uncertainties are shown in Figure 2. We will compare the inferred concentrations in these species to available data and two-dimensional models in the discussion section which follows.

Altitude dependence of the inferred concentrations is shown in Figure 3, in which we consider the latitudes 5°, 35°, and 65°N. A number of features are apparent from Figure 3. First, each species has a different and characteristic altitude dependence, which, in general, does not vary enormously from one month to the next. Second, seasonal dependence is least at

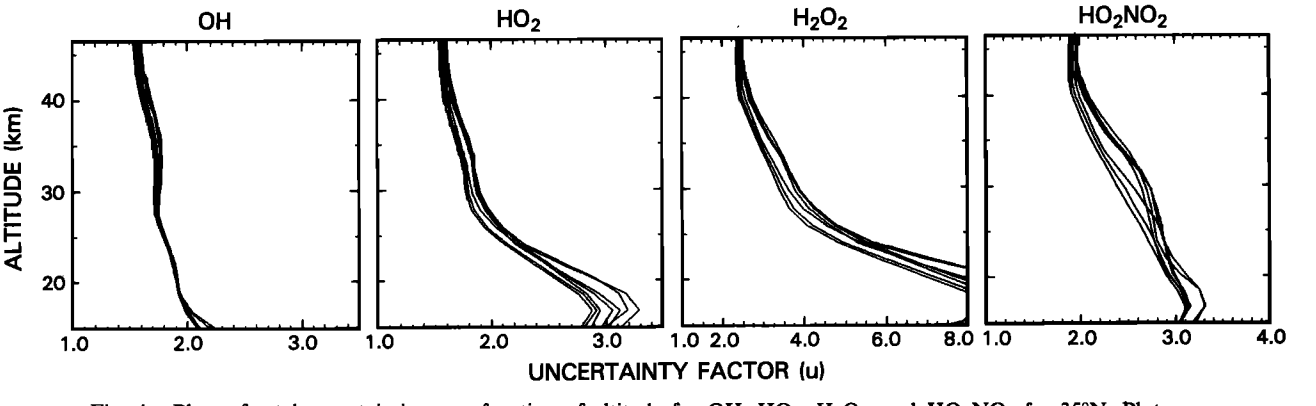

Fig. 4. Plots of total uncertainties as a function of altitude for OH, HO_2, H_2O_2, and HO_2NO_2 for 35°N. Plots are arranged as are those in Figure 3.

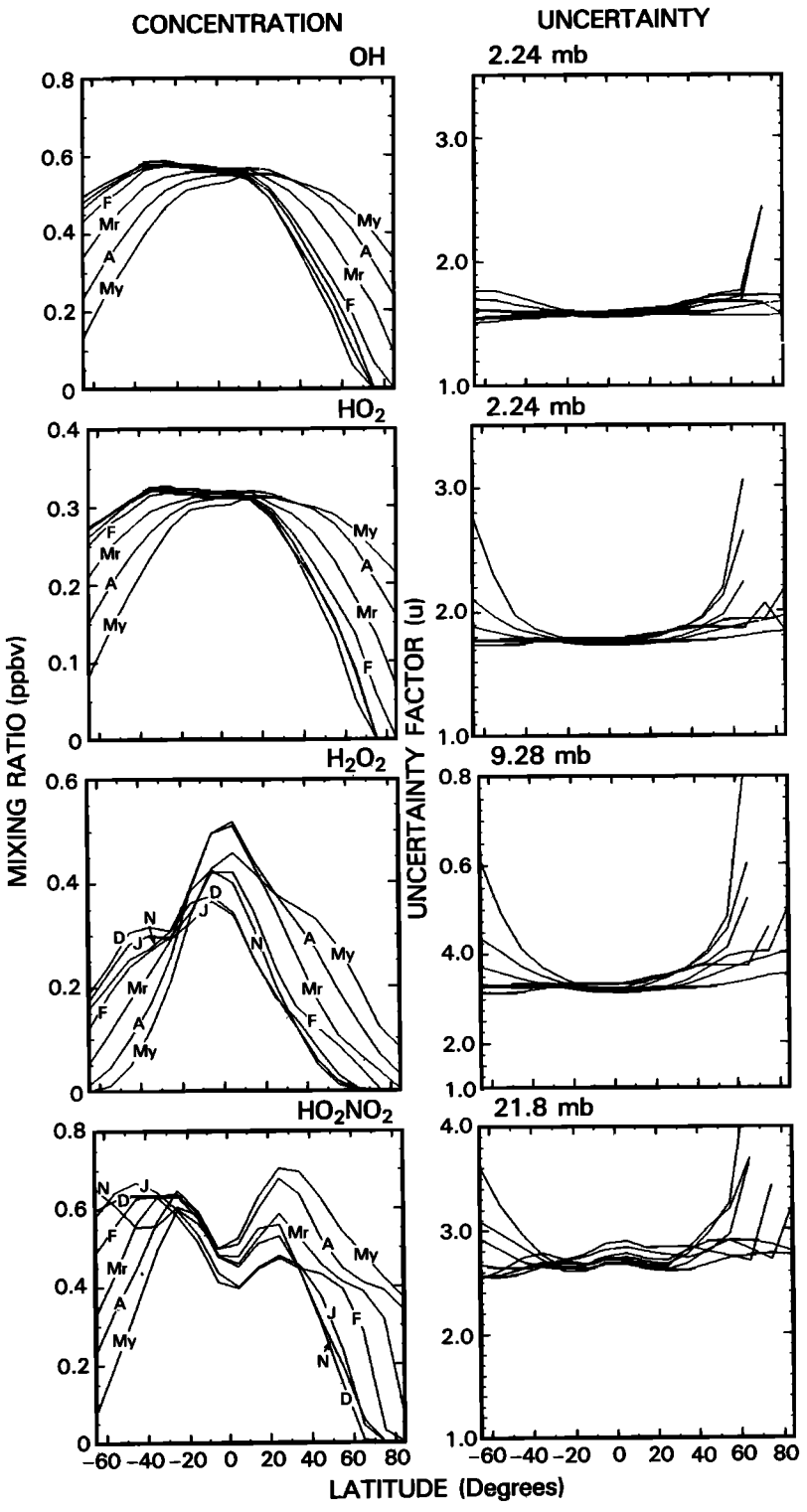

Fig. 5. Plots of mixing ratios (left column) and total uncertainties (right column) for OH (top row), HO_2 (second row), H_2O_2 (third row), and HO_2NO_2 (fourth row) at the pressure levels indicated. Curves are lettered as in Figure 4.

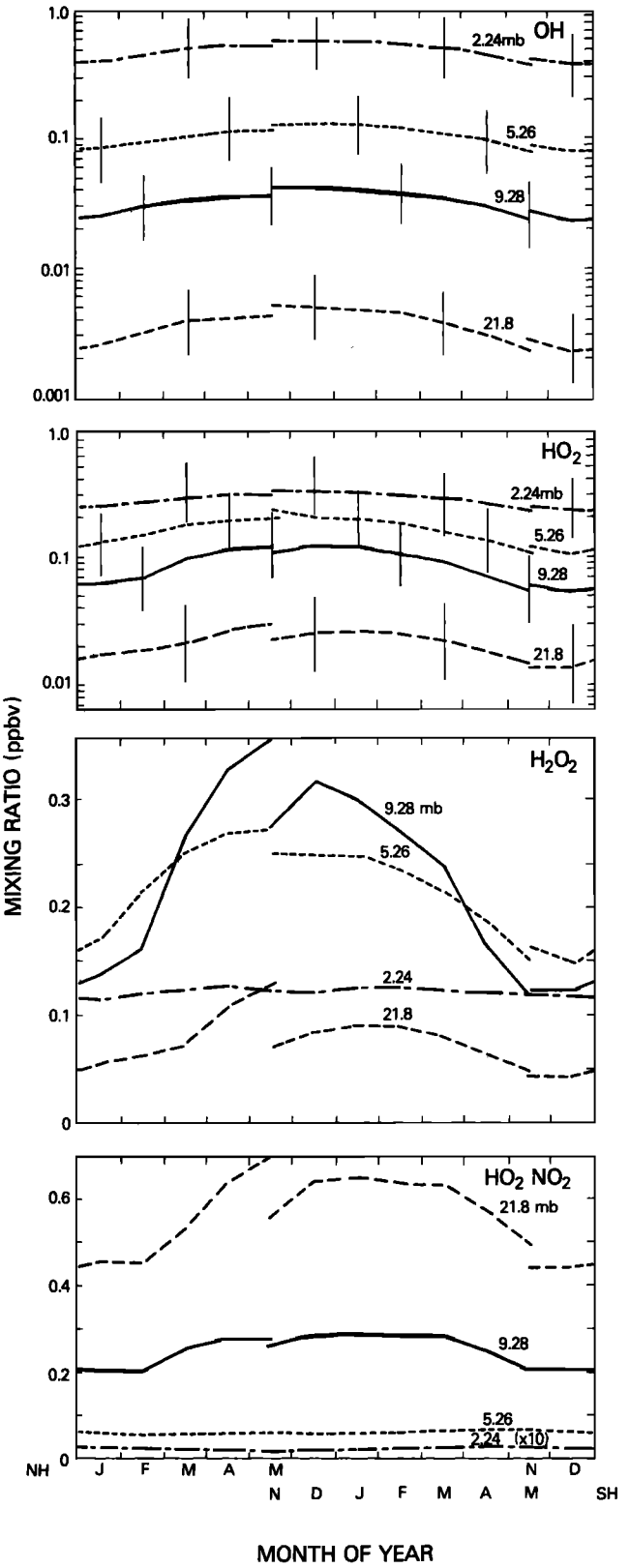

Fig. 6. Plots of mixing ratios at 35° as a function of month for, reading down, OH, HO_2, H_2O_2, and HO_2NO_2. Line types correspond to the pressure levels centered about the values indicated: 21.8 mbar (dashed line), 9.28 mbar (solid line), 5.26 mbar (dotted line), and 2.24 mbar (dashed-dotted line). Data plotted from May to November on the northern hemisphere (NH) abscissa are southern hemisphere (SH) values displaced by 6 months as described in the text. Error bars indicated for OH and HO_2 correspond to total uncertainties. Note that OH and HO_2 plots have logarithmic ordinates.

5°N and largest at 65°N. Third, OH is seen to have the least month-to-month variability in the tropics and mid-latitudes, while H_2O_2 is seen to have the largest. Uncertainties for these species are plotted as a function of height for 35°N in Figure 4, and as with the concentrations, each species not only has a reasonably different and characteristic profile, but also the monthly variability in the uncertainty is smallest for OH.

Some measure of the monthly variation in the latitude dependence of the inferred concentrations and their uncertainties may be seen in Figure 5, in which the concentrations and uncertainties are plotted as a function of latitude for each month. Plots for H_2O_2 and HO_2NO_2 are for pressure levels close to those at which each species reaches its maximum mixing ratio (see Figure 1). Focusing on the concentrations (left-hand side of Figure 5), we see several important features. First, each species displays its own characteristic shape. Second, there is a very apparent seasonal shift in the profiles of all the species in that they tend to have higher values in regions of greater sunlight (for example, southern hemisphere summer) than they do in the more dimly lit regions. Third, for most of the species (least so for OH), as one approaches the terminator, there are dramatic reductions in the concentration of the inferred species. Since the photochemical equilibrium approximation used begins to break down in these regions, the exact magnitude of the falloff may not be correctly represented.

Comparing the concentration and uncertainty plots in Figure 5, one sees three major features of interest. First, in mid-latitudes the uncertainties vary much less rapidly with latitude than do the concentrations, especially for H_2O_2 and HO_2NO_2. Second, as one approaches the terminator, uncertainties get larger while the concentrations become small. Third, in mid-latitudes, again primarily for H_2O_2 and HO_2NO_2, there is considerably less monthly variation in the uncertainties than there is in the concentrations.

To further consider the annual variation of these species at mid-latitudes (35°), we plot their concentrations as a function of month of the year in Figure 6. We show the pressure levels centered at 21.8, 9.28, 5.26, and 2.24 mbar, respectively. Since there are only 7 months of LIMS data, we fill in the missing months by using 35°N and 35°S data together, assuming that 35°S November data can be treated as 35°N May data, and keeping this 6-month phase difference for all 7 months of data. This treatment will lead to two data points for May and November, and the difference between the two different values in each of those months may be indicative of differences between the northern and southern hemispheres or of errors in the model input. Error bars, corresponding to the total uncertainties, are shown for OH and HO_2 in Figure 6 for 4 months for each of the pressure levels. Uncertainties in the four species are plotted in Figure 7 in a manner similar to that in which the concentrations were plotted in Figure 6.

The major features of interest in Figure 6 and 7 are as follows. First, we see for all species a late spring-summertime concentration or mixing ratio maximum, although this is somewhat weaker for OH than it is for the other species. This variation is, in general, smaller than the uncertainty in the inferred values, however. Second, for some species and altitudes we see a sizable difference between the 35°N May and 35°S November values. In general, the difference between the 35°N November and 35°S May values are smaller. In spite of these differences the seasonal behavior remains clear. Third, we see a considerably smaller variation in the total uncertainties than we do in the concentrations. This is especially true for HO_2 at the 9.28- and 5.26-mbar pressure levels.

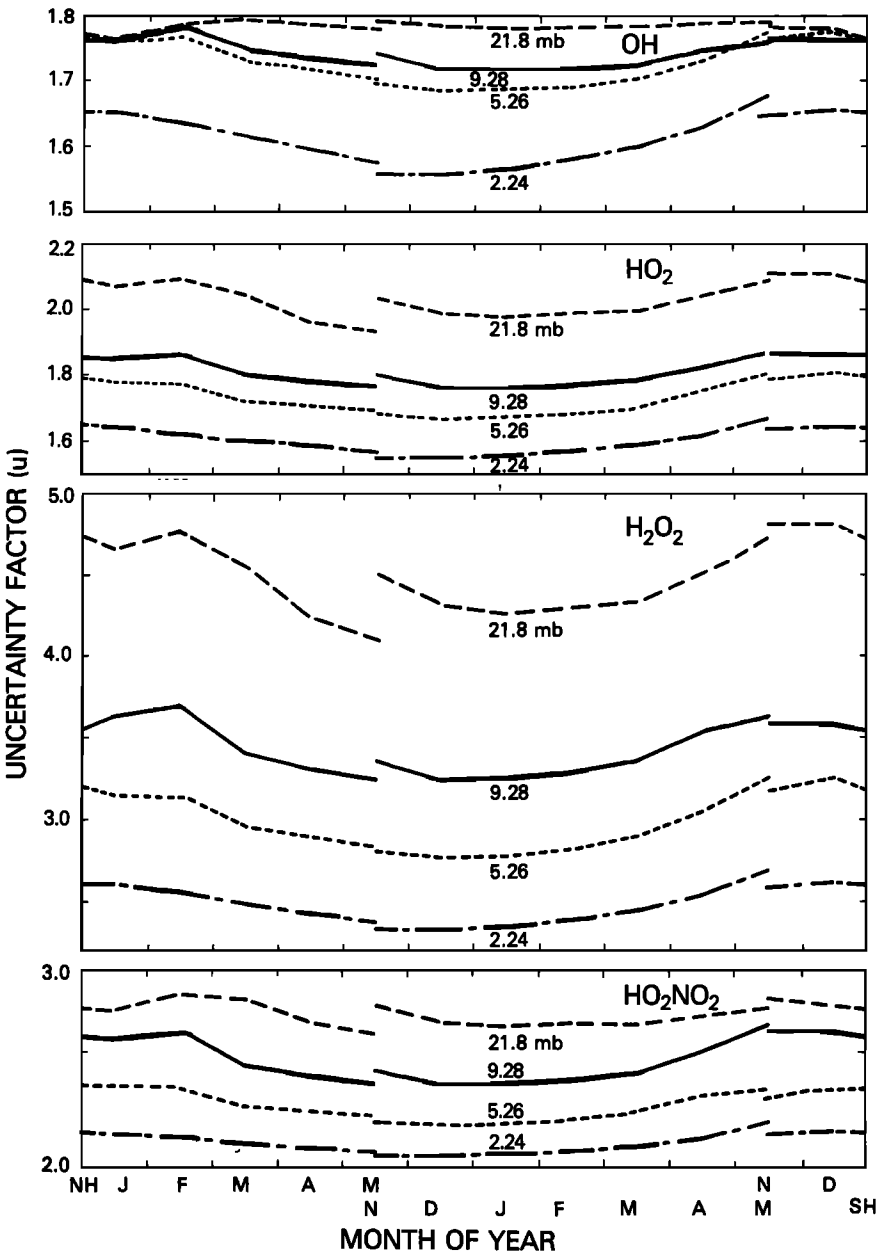

Fig. 7. Plots of uncertainties at 35° latitude as a function of month for, reading down, HO_2, H_2O_2, and HO_2NO_2. Line types and significance are as in Figure 6.

4. Discussion

In this section we will compare the inferred concentrations of OH, HO_2, H_2O_2, and HO_2NO_2 with available observational data as well as the results of two-dimensional models. We are particularly interested in the overlap, if any, of the inferred concentrations, taking into account their estimated uncertainties, and the observed concentrations, also taking into account their uncertainties. We will also comment on the variation of the uncertainties with latitude and time and the difference between their variation and that of the inferred concentrations. We first consider the available observations and then examine some of the more recent and comprehensive two-dimensional photochemical models.

Comparison With Observations

The data base of observations of concentrations of OH, HO_2, H_2O_2, and HO_2NO_2 is very limited, with the greatest amount of information being available for OH and the least being available for HO_2NO_2 [*WMO*, 1982]. As mentioned earlier, the best studied latitude range is 30°–40°N, as Palestine, Texas, the launching point for most American balloon flights, is at 32°N. Balloon-borne experiments launched from Palestine have been used for the detection of OH [*Anderson*, 1976, 1980; *Heaps and McGee*, 1983, 1985], HO_2 [*Anderson et al.*, 1981], and H_2O_2 [*Waters et al.*, 1981; *Chance and Traub*, 1984]. For this reason, in comparing our inferred concentrations for OH and HO_2 with observed ones, we will, in general, plot our 35°N data; to further simplify such comparison plots, we will plot only the March data, as these should be in the middle of the annual range of concentrations (see Figure 6). Lines showing the monthly averaged concentration and this value multiplied and divided by the calculated uncertainties are also shown. Such plots are presented for OH in Figure 8, HO_2 in Figure 9, H_2O_2 in Figure 10 (since the only

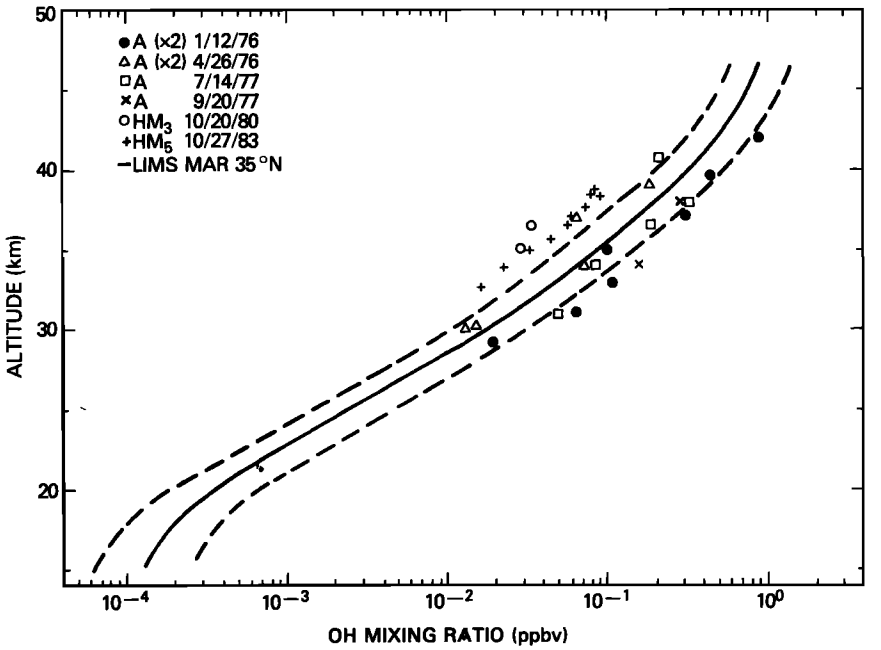

Fig. 8. Plot of inferred OH mixing ratio (in ppbv) versus height. Solid line corresponds to 35°N monthly zonal average for March; dashed lines are limits given from combining calculated concentrations and uncertainties as described in the text. Symbols correspond to observations noted with the abbreviations A for *Anderson* [1971, 1976, 1980], HM_3 for *Heaps and McGee* [1983], and HM_5 for *Heaps and McGee* [1985]. Estimated uncertainties are 30% for the later measurements of *Anderson* [1976, 1980], 50% for *Anderson*'s [1971] earlier measurement, and 130% for *Heaps and McGee* [1983]. See text for discussion of uncertainty of *Heaps and McGee* [1985] data. Some observational results have been multiplied by two (×2) before plotting to account for diurnal effects [*WMO*, 1982].

observation of H_2O_2 plotted in Figure 10 is for January, we plot the inferred monthly averaged value for that month).

There is appreciable scatter in the OH measurements, as may be seen from the data points plotted in Figure 8. Some of the scatter could be due to differences in [OH] over the course of a year, but the general absence of any systematic difference suggests that local short-term variability and/or experimental uncertainty may be responsible for the scatter. The estimated uncertainty (30%) in the measurements of *Anderson* [1976, 1980] is not sufficiently large to account for the nearly fivefold

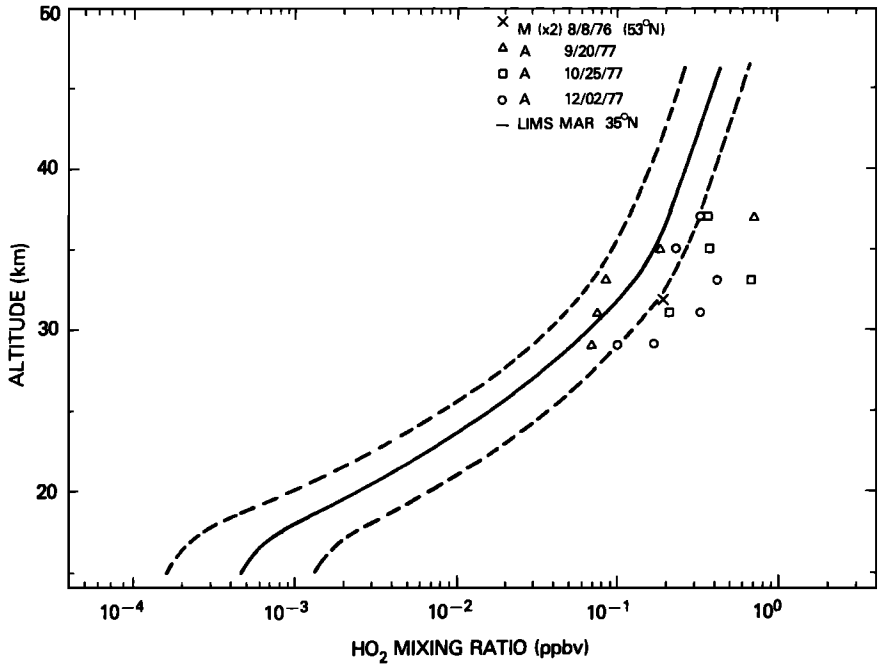

Fig. 9. Plot of inferred HO_2 mixing ratio (in ppbv) versus height for 35°N in March. Solid and dashed lines are concentrations and uncertainty limits, respectively, as described in the caption for Figure 8. Symbols correspond to observations noted with the abbreviations A for *Anderson et al.* [1981] and M for *Mihelcic et al.* [1978]. Note that the latter measurement is from 53°N and has been multiplied by two (×2) before plotting to account for diurnal effects [*WMO*, 1982].

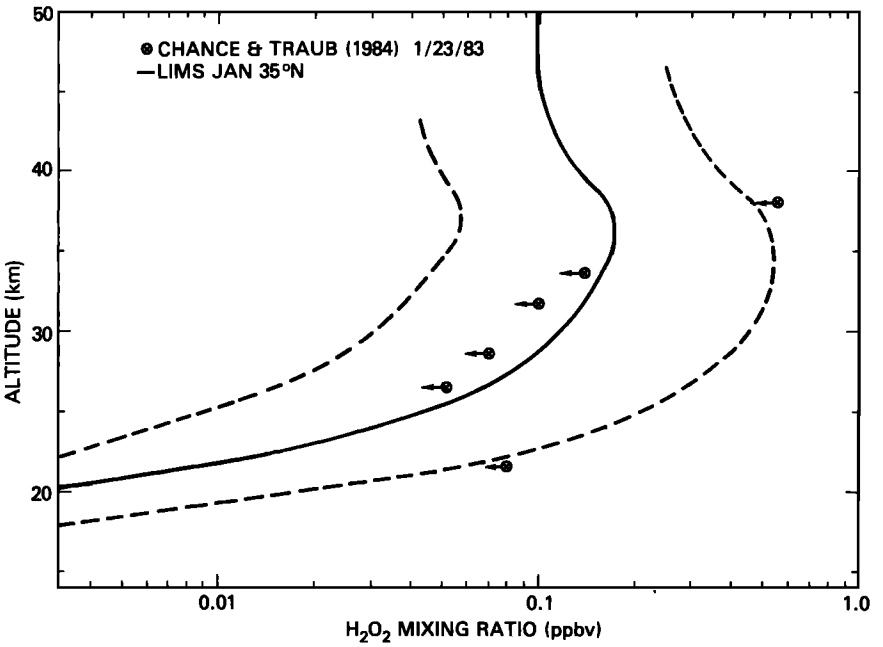

Fig. 10. Plot of inferred H_2O_2 mixing ratio (in ppbv) versus height for 35°N in January. Solid and dashed lines are concentrations and uncertainty limits, respectively, as described in the caption for Figure 8. Symbols correspond to upper limits taken from Table 1 of *Chance and Traub* [1984].

difference between the two 37 km data of Anderson shown in Figure 8. In general, the uncertainty in the measurements is sufficiently large, however, that there is appreciable overlap of the allowable range of inferred OH concentrations with that of the error bars associated with the observations. There is considerably less overlap with the data of *Heaps and McGee* [1983], however. They quote a value of $(4.9 \pm 6.4) \times 10^6$ cm^{-3} for [OH] using their direct method for the local time 1347–1410 CDT in the altitude range from 34 to 36 km. In examining the data of *Heaps and McGee* [1983], one must allow for the diurnal variation in OH, as the observations were made somewhat after local noon (1347–1534 local time) and should thus be somewhat smaller than the corresponding local noon values such as have been inferred here [*Fabian et al.*, 1982].

The more recent data of *Heaps and McGee* [1985] (converted to mixing ratios for plotting by using number densities from the U.S. Standard Atmospheres, 1976) lead to higher values of [OH] than their earlier measurements but are still somewhat below the values inferred here. The error estimates for their later results are much smaller than their earlier ones (approximately $\pm 0.5 \times 10^6$ cm^{-3} for the later data). Since these data are from late October, when [OH] is expected to be slightly lower than in March, some of the difference may be due to seasonal effects.

There have also been numerous measurements of the total atmospheric OH column measured from the ground by studying the resonance absorption of sunlight by OH [*Burnett*, 1976; *Burnett and Burnett*, 1981, 1982, 1984]. These measurements suggest that the total OH column is of the order of 5.7×10^{13} cm^{-2} with an uncertainty of 25% at midday at 40°N [*WMO*, 1982]. A direct comparison of these OH column measurements with those which may be obtained from the individual OH measurements presented here should be made with extreme caution, as the total atmospheric OH column should contain a major contribution from mesospheric OH and a minor (perhaps negligible) one from tropospheric OH. *Allen et al.* [1981, 1984], in their one-dimensional photochemical modeling studies, estimated OH concentrations which lead to a mesospheric column of some 3×10^{13} cm^{-2}, corresponding to nearly one half of the expected total column. A tropospheric column not appreciably above 3×10^{12} cm^{-2} at mid-latitudes may be inferred from the OH concentrations obtained by *Crutzen and Gidel* [1983] in their two-dimensional tropospheric photochemical model.

From the calculations performed here, we can obtain approximate OH columns for the altitude region from 14.9 to 46.4 km, which corresponds to the centers of pressure levels 8–24 of the Goddard two-dimensional diabatic circulation model [*Guthrie et al.*, 1984*a*]. These are plotted as a function of the solar zenith angle χ in Figure 11, as good correlations have been observed between these two quantities [*Burnett and Burnett*, 1981, 1982, 1984]. The data plotted in Figure 11 do not precisely correspond to that of Burnett and Burnett, however, as they observed OH at one fixed latitude and achieved their solar zenith angle variation by allowing for changes in day and local time, while our data are for a variety of latitudes and days but are all for a local time of noon. Only solar zenith angles smaller than 63° are shown, as at larger angles the assumption of local noon in calculating photolysis rates becomes less appropriate due to the fact that the LIMS viewing time does not precisely correspond to local noon.

The general features of OH versus sec χ in Figure 11 are similar in the works of *Burnett and Burnett* [1981, 1984] except that there is perhaps less of a cusp at $\chi = 1$ in our figure than they obtained. There also appears to be some systematic difference between the northern hemisphere results for November through January and those of other months. This difference is considerably smaller than the uncertainty in the inferred OH column, however. The total amount of OH seen is somewhat over half the composite value of 6.9×10^{13} cm^{-2} inferred from in situ measurements [*WMO*, 1982] (a

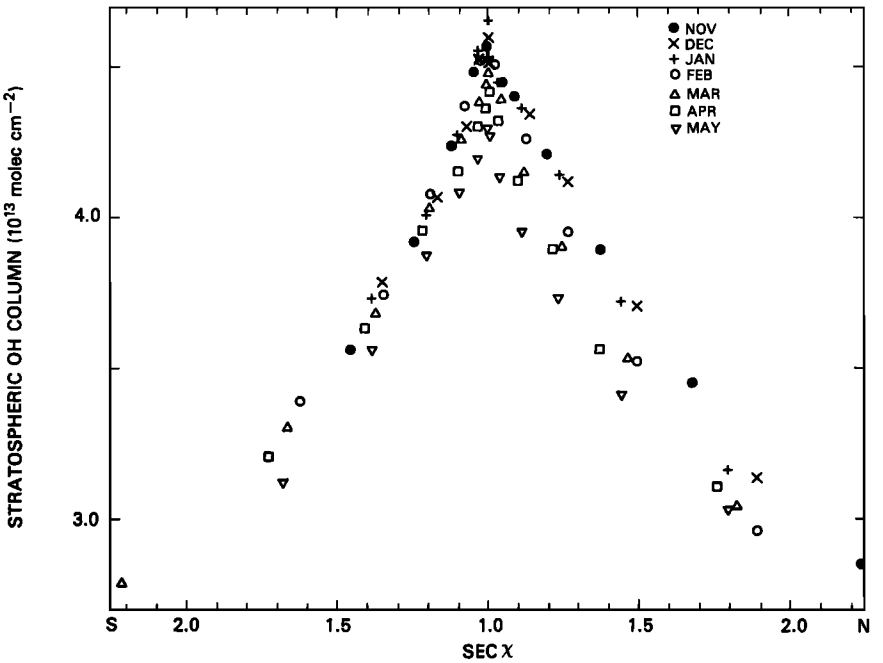

Fig. 11. Column abundance of OH inferred from LIMS data as a function of the solar zenith angle χ. Symbols correspond to months as indicated. Data to left of center (sec $\chi = 1.0$) are from latitudes south (S) of latitudes where the sun is directly overhead at noon; those to the right are from latitudes to the north (N).

slightly larger value would be expected at 35°N). Thus the OH column inferred here for the major portion of the stratosphere is compatible with the total OH column abundance measurements of *Burnett and Burnett* [1981, 1982, 1984] and that inferred from the in situ measurements [*WMO*, 1982].

There is somewhat less agreement between the HO_2 concentrations inferred here and the available observational data than there is for OH, as may be seen from Figure 9. With some exceptions, the $[HO_2]$ observations of *Anderson et al.* [1981] are considerably above the values inferred here, although the uncertainty in the measurements (45%) is sufficiently large that many of the error bars will overlap the concentration range permitted by the uncertainties in the inferred species' concentrations. The uncertainty in the measurement of *Mihelcic et al.* [1978] is very large (factor of 3) and thus has substantial overlap with the concentration range shown in Figure 9. Since their data are for 53°N in August, comparison with 35°N in March is probably reasonable, as the expected decrease in HO_2 with latitude (see Figure 1) should be at least partially offset by the expected higher value of HO_2 in August than in March (see Figure 6).

Recently, *de Zafra et al.* [1984] presented results of a millimeter-wave measurement of stratospheric HO_2 at 19.5°N in September and October 1982. While they did not invert their results to produce an HO_2 profile, they do show that the high HO_2 values measured by *Anderson et al.* [1981], when combined with upper stratospheric and mesospheric HO_2 determined in photochemical model calculations, would lead to line shapes and intensities different from those measured. Because of the relative insensitivity of their technique to HO_2 below 35 km, this is not a strong conclusion, however. Nevertheless, their apparent indication that lower values of midstratospheric (30–35 km) HO_2 than were measured by *Anderson et al.* [1981] are required is consistent with the HO_2 profiles inferred here.

For H_2O_2 the only published measurements are those of *Waters et al.* [1981] and of *Chance and Traub* [1984]. The latter authors also cite deZafra et al. (unpublished manuscript, 1983). *Waters et al.* [1981] determined an approximate mixing ratio of 1.1 ppbv for H_2O_2 near 32 km at 32°N in February 1981. This is substantially above the values (0.15–0.2 ppbv) inferred here, even allowing for the estimated factor of 3.5 uncertainty (see Figure 4).

Chance and Traub [1984] measured appreciably smaller values in January 1983, also at 32°N. They determined upper limits for $[H_2O_2]$ below 0.1 ppbv below 32 km; their highest upper limit was 0.52 ppbv at 38 km. They note that the shape of their upper limit profile may be more a reflection of the sensitivity of their technique than it is of the actual stratospheric H_2O_2 profile. Their upper limits are quite compatible with the concentrations and uncertainties inferred here.

Chance and Traub [1984] also reference millimeter-wave measurements of R. L. de Zafra et al. (unpublished data, 1983) (as cited by *Chance and Traub* [1984]) from May to June 1983, which are indicative of a mean mixing ratio of 0.4–0.6 ppbv above 30 km. These latter results compare favorably with those inferred here from LIMS data. The much larger values observed by de Zafra et al. should be due mainly to the large increase in H_2O_2 expected as one approaches the summer solstice (see Figure 6), with a minor contribution due to the expected increase as one goes from the 32°N latitude of Palestine, Texas, to the 19.5°N latitude of Mauna Kea, Hawaii, from where the millimeter-wave measurements were made.

As indicated earlier, the only published observation of HO_2NO_2 is an upper limit of 0.4 ppbv by Murcray and coworkers reported by *NASA* [1979]. While some of our inferred concentrations are greater than this, they are at altitudes considerably below the 40 km altitude at which the infrared spectrum used to obtain this upper limit was taken. Their technique did observe lower levels, however, but the difficulties expected in the observations should not necessarily

cause one to reject our higher values as being incompatible with the cited upper limit.

Comparison With Photochemical Models

There are several two-dimensional models with which results might be compared. These differ in their treatment of dynamics and chemistry, although those of the latter are usually due to a different choice of standard reaction rates, i.e., *WMO* [1982] used by *Ko et al.* [1984] and *DeMore et al.* [1981] used by *Miller et al.* [1981] and by *Garcia and Solomon* [1983] and *Solomon and Garcia* [1983]. We note that each of these have a few different reaction rates, mainly for HO_x reactions, from the *DeMore et al.* [1983] rates used here. Because of the somewhat greater availability of OH and HO_2 observational data and of previous work comparing their concentrations inferred from LIMS data with observations [*Jackman et al.*, 1985*a*; *Pyle and Zavody*, 1985; KJ], we will restrict the comparison of model and inferred results to the species H_2O_2 and HO_2NO_2. Unfortunately, *Ko et al.* [1984] in reporting the results of their two-dimensional modeling project do not present results for these species, so we are forced to compare our results with the earlier models cited above.

Miller et al. [1981] obtained a maximum mixing ratio of near 0.4 ppbv for H_2O_2 in April occurring over the equator near 30 km. Our calculations yielded an April maximum of 0.55 ppbv, also near 30 km above the 0°–10°N latitude region. *Miller et al.* [1981] also noted that at 20 km they calculated H_2O_2 to be present at less than 0.1 ppbv for all latitudes and seasons. This is entirely consistent with our results (see Figure 1), even with the very large uncertainty (factor of 7) we estimate for H_2O_2 at the 20-km level.

Garcia and Solomon [1983] presented results for H_2O_2 close to the winter solstice. They obtained a maximim H_2O_2 concentration of between 3×10^8 and 1×10^9 cm^{-3} near 30 km from 0° to 40°S. At the 32 km, 32°N measurement location of *Waters et al.* [1981], they calculated a winter solstice mixing ratio of 0.3 ppbv, considerably below the 1.1 ppbv found by *Waters et al.* [1981] in February and somewhat above the 0.10–0.15 ppbv values inferred here.

Connell et al. [1985] have noted that extremely large variability in stratospheric H_2O_2 (a factor of 4–5) may be expected based on the variation of O_2, H_2O, NO_2, NO, and HNO_3. With the exception of NO, these are the LIMS observables; NO may be simply calculated given the LIMS NO_2, O_3, and T fields. Thus it is probably unwise to stress any one measurement very much, as it may not be a reflection of the "average" atmosphere. The large variability they infer is intimately related to the large uncertainty we calculate, as both require large sensitivity coefficients.

Somewhat less attention has been given to the distribution of HO_2NO_2 in the atmosphere. *Miller et al.* [1981] calculated maximum mixing ratios of approximately 1 ppbv occurring uniformly over latitude at an altitude of 30 km. We inferred peak mixing ratios of the order of 0.6–0.8 ppbv, occurring primarily in mid-latitudes, although the latitude dependence is fairly weak away from the poles, at altitudes between 25 and 30 km. *Solomon and Garcia* [1983] displayed curves of concentrations of calculated HO_2NO_2 profiles at 32°N and 54°N for winter solstice conditions. Their peak values, corresponding to mixing ratios of 0.75–0.8 ppbv at 32°N and 0.5 ppbv at 54°N, are somewhat greater than our December values. Some of the difference is undoubtedly due to their use of the slow *DeMore et al.* [1981] value for $k_{OH+HO_2NO_2}$ of 8×10^{-13} cm^3 molecule^{-1} s^{-1}, while we used the faster *DeMore et al.* [1983] value of $1.3 \times 10^{-12} \exp(380/T)$ cm^3 molecule^{-1} s^{-1}. Near 25 km, this newer rate is a factor of 9 higher than the older one. Lower values of HO_2NO_2 have been inferred in the one-dimensional model of *Connell et al.* [1985], which uses the newer rate for $k_{OH+HO_2NO_2}$.

Thus, in general, the inferred concentrations of H_2O_2 and HO_2NO_2 are consistent with the results of some recent two-dimensional models, especially considering the large uncertainties in the model input parameters.

Uncertainties and Their Variation With Latitude and Season

The magnitude of the uncertainties u_i, in general, decreases in the order $u_{H_2O_2} > u_{HO_2NO_2} > u_{HO_2} > u_{OH}$ (see Figure 4), although in the upper stratosphere, u_{HO_2} and u_{OH} are equivalent, as are $u_{HO_2NO_2}$ and u_{HO_2} in the lower stratosphere. The origins of the differing altitude behavior of u_{OH} and u_{HO_2} have been discussed in some detail in our previous work (KJ) and may be briefly summarized by noting that HO_2 is extremely sensitive to O_3 and NO_2 in the lower stratosphere, while OH is not, and that NO_2, in particular, has very large uncertainties in the lower stratosphere. Also, the low temperatures in the lower stratosphere lead to larger uncertainties in the reaction rates than in the warmer, upper stratosphere.

The very large uncertainty in H_2O_2 is due mainly to the fact that sensitivity coefficients for H_2O_2 are twice as large as those for HO_2. This occurs because of the logarithmic nature of the sensitivity coefficients. Neglecting the reaction

$$OH + H_2O_2 \rightarrow H_2O + HO_2 \tag{21}$$

one has

$$[H_2O_2] = k_{23}[HO_2]^2/J_{24} \tag{22}$$

where k_{23} and J_{24} are the rates of the processes

$$2HO_2 \rightarrow H_2O_2 + O_2 \tag{23}$$

and

$$H_2O_2 + h\nu \rightarrow 2OH \tag{24}$$

respectively. Thus one sees

$$\ln [H_2O_2] = 2 \ln [HO_2] + \ln k_{23} - \ln J_{24} \tag{25}$$

so the logarithmic derivatives of H_2O_2 should be twice those of HO_2 with respect to the corresponding input parameter. In calculating uncertainties by (20), we see that on replacing all S_{ij} by $2S_{ij}$, the corresponding uncertainty u_i is replaced by its square. This dependence may be seen by comparison of u_{HO_2} and $u_{H_2O_2}$ in Figure 3 or in Figure 4.

The uncertainty of HO_2NO_2 is larger than that of HO_2 through most of the stratosphere because of its large sensitivity to the reactions which produce and destroy HO_2NO_2 ($k_{OH+HO_2NO_2}$, $k_{HO_2+NO_2+M}$, $J_{HO_2NO_2}$), all of which have fairly large uncertainties [*DeMore et al.*, 1983]. The near equivalence of u_{HO_2} and $u_{HO_2NO_2}$ in the lower stratosphere is due mainly to the fact that for this model, $[HO_2NO_2]$ is relatively independent of $[NO_2]$ in the lower stratosphere because $[HO_2]$ and $[NO_2]$ are themselves inversely proportional. This inverse proportionality occurs because the major stratospheric loss process for HO_2 is (equation (10))

$$HO_2 + NO \rightarrow OH + NO_2$$

where NO is proportional to NO_2 for a given NO_2 con-

centration. Thus HO_2NO_2 formation becomes the product of a term inversely proportional to NO_2 and of NO_2 itself, so that it becomes essentially NO_2 independent. In the lower stratosphere, then, the large uncertainty in NO_2 becomes unimportant. As one goes to higher altitudes and $O + HO_2 \rightarrow OH + O_2$ becomes an important loss process for HO_2, the dependence of $[HO_2]$ on $[NO_2]$ becomes less than an inverse one, and the uncertainty in NO_2 begins to contribute to the HO_2NO_2 uncertainty. Thus, in the mid-stratosphere, $u_{HO_2NO_2} > u_{HO_2}$.

One of the more interesting results to come from this study is the fact that the calculated uncertainties have considerably less variation with latitude and, to a lesser extent, season than do the concentrations. This may be seen very clearly for latitudinal variation in Figure 4, where in the tropics and mid-latitudes there is little if any latitude dependence for uncertainties, while there is substantial dependence for concentrations. Latitude dependence becomes important only as one gets close to the poles, especially the winter pole. Thus for mid-latitudes one may assume latitude and season independent uncertainties away from the winter pole without appreciable error. Close to the terminator, where uncertainties become large, the photochemical equilibrium approximation used becomes less appropriate, and the results are expected to be at best qualitatively correct, anyhow.

Uncertainties are derived from two types of quantities: sensitivity coefficients calculated with the algebraic photochemical equilibrium model and model input parameter uncertainties supplied with the input data. Since the latter are just a set of constants (we assume the uncertainty in the input concentrations to vary only with altitude and not with latitude or season), the relative constancy of the uncertainties reflects relative constancy of the sensitivity coefficients. Thus tables of sensitivity coefficients, such as those shown in our previous work (KJ), should not change appreciably over the year. This will simplify the use of sensitivity coefficients to study short-term and local variability of inferred species concentrations, as one essentially needs to consider only the variability of the model input; a table of sensitivity coefficients which vary only with altitude may be used for all mid-latitude locations over all seasons.

5. CONCLUSIONS

We have shown that zonally and monthly averaged LIMS data and our algebraic photochemical equilibrium model described previously (KJ) can be used to infer concentrations of the odd hydrogen species OH, HO_2, H_2O_2, and HO_2NO_2 as a function of altitude, latitude, and season. By comparing the inferred concentrations together with their uncertainties with observed distributions of OH, we see that with the exception of the early OH observations of *Heaps and McGee* [1983], the inferred OH concentration and the measured values appear to be compatible. For HO_2, however, the inferred values in the 30–35 km range are appreciably lower than the values measured by *Anderson et al.* [1981]. For H_2O_2 the inferred values are quite consistent with recent measurements of *Chance and Traub* [1984], although they are substantially below those of *Waters et al.* [1981]. Since the latter obtained values which are above those of the other observations and of most models, that difference is not especially surprising. For HO_2NO_2 the maximum mixing ratios calculated are all below 1 ppbv, although values greater than the one measured upper limit of 0.4 ppbv were calculated. We have demonstrated the expected variation of these quantities with latitude, altitude, and season and shown that at mid-latitudes, where most observations have been made, they are expected to maximize in the summer.

Uncertainties are found to decrease in the order $u_{H_2O_2} > u_{HO_2NO_2} > u_{HO_2} > u_{OH}$, although in the upper stratosphere u_{HO_2} and u_{OH} are roughly equal, as are $u_{HO_2NO_2}$ and u_{HO_2} in the lower stratosphere. The variation of the uncertainties with latitude and season is, in general, substantially smaller than that of the concentrations. Their variation with latitude is frequently systematic of variations in important chemical processes with altitude.

The algebraic nature of the model allows one to easily see to first order the effect of variation of any model input parameter (concentration, rate coefficient, uncertainty) or its uncertainty on the inferred concentration of the HO_x species and their uncertainties. Such relationships may prove useful in the planning of future field and laboratory measurements. The sensitivity coefficients, as described earlier, not only are helpful in intuitively understanding the chemistry of the stratosphere but should prove to be very useful in studying the short-term and local variability of inferred species concentrations.

Acknowledgments. We thank M. A. Geller and R. S. Stolarski for their help, advice, and support of this work and for their comments on an earlier version of this manuscript. We thank W. S. Heaps, K. V. Chance, D. Wuebbles and P. Connell, and J. Pyle for sending us preprints of their work. We also thank Roberta M. Duffy for her assistance in the preparation of this manuscript. Contribution 27 of the Stratospheric General Circulation with Chemistry Modeling Project at NASA Goddard Space Flight Center.

REFERENCES

Allam, R. J., K. S. Groves, and A. F. Tuck, Global OH distribution derived from general circulation model fields of ozone and water vapor, *J. Geophys. Res.*, *86*, 5303–5320, 1981.

Allen, M., Y. L. Yung, and J. W. Waters, Vertical transport and photochemistry in the terrestrial mesosphere and lower thermosphere (50–120 km), *J. Geophys. Res.*, *86*, 3617–3627, 1981.

Allen, M., J. I. Lunine, and Y. L. Yung, The vertical distribution of ozone in the mesosphere and thermosphere, *J. Geophys. Res.*, *89*, 4841–4872, 1984. (Correction, *J. Geophys. Res.*, *89*, 11827, 1984.)

Anderson, J. G., Rocket measurement of OH in the mesosphere, *J. Geophys. Res.*, *76*, 7820–7824, 1971.

Anderson, J. G., The absolute concentration of $OH(X^2\Pi)$ in the earth's stratosphere, *Geophys. Res. Lett.*, *3*, 165–168, 1976.

Anderson, J. G., Free radicals in the Earth's stratosphere: A review of recent results, in *Proceedings of the NATO Advanced Study Institute on Atmospheric Ozone*, edited by A. C. Aikin, pp. 233–251, U.S. Department of Transportation, Federal Aviation Administration, Washington, D. C., 1980.

Anderson, J. G., H. J. Grassl, R. E. Shetter, and J. J. Margitan, HO_2 in the stratosphere: Three in situ observations, *Geophys. Res. Lett.*, *8*, 289–292, 1981.

Barth, C. A., D. W. Rusch, R. J. Thomas, G. H. Mount, G. J. Rottman, G. E. Thomas, R. W. Sanders, and G. M. Lawrence, Solar mesosphere explorer: Scientific objectives and results, *Geophys. Res. Lett.*, *10*, 237–240, 1983.

Burnett, C. R., Terrestrial OH abundance measurement by spectroscopic observation of resonance absorption of sunlight, *Geophys. Res. Lett.*, *3*, 319–322, 1976.

Burnett, C. R., and E. B. Burnett, Spectroscopic measurement of the vertical column abundance of hydroxyl (OH) in the earth's atmosphere, *J. Geophys. Res.*, *86*, 5185–5202, 1981.

Burnett, C. R., and E. B. Burnett, Vertical column abundance of atmospheric OH at solar maximum from Fritz Peak, Colorado, *Geophys. Res. Lett.*, *9*, 708–711, 1982.

Burnett, C. R., and E. B. Burnett, Observational results on the vertical column abundance of atmospheric hydroxyl: Description and its seasonal behavior 1977–1982 and of the 1982 El Chichon perturbation, *J. Geophys. Res.*, *89*, 9603–9611, 1984.

Butler, D. M., The uncertainty in ozone calculations by a stratospheric photochemistry model, *Geophys. Res. Lett.*, *5*, 769–772, 1978.

Butler, D. M., Input sensitivity study of a stratospheric photochemistry model, *Pure Appl. Geophys.*, *117*, 430–435, 1979.

Chance, K. V., and W. A. Traub, An upper limit for stratospheric hydrogen peroxide, *J. Geophys. Res.*, *89*, 11655–11660, 1984.

Connell, P. S., D. J. Wuebbles, and J. S. Chang, Stratosphere hydrogen peroxide: The relationship of theory and observation, *J. Geophys. Res.*, *90*, 10,726–10,732, 1985.

Crutzen, P. J., and L. T. Gidel, A two-dimensional photochemical model of the atmosphere, 2, The tropospheric budgets of the anthropogenic chlorocarbons, CO, CH_4, CH_3Cl and the effect of various NO_x sources on tropospheric ozone, *J. Geophys. Res.*, *88*, 6641–6661, 1983.

DeMore, W. B., and Y. L. Yung, Catalytic processes in the atmospheres of Earth and Venus, *Science*, *217*, 1209–1213, 1982.

DeMore, W. B., D. M. Golden, R. F. Hampson, C. J. Howard, M. J. Kurylo, M. J. Molina, A. R. Ravishankara, and R. T. Watson, Chemical kinetic and photochemical data for use in stratospheric modeling: Evaluation number 4, *JPL Publ.*, *81-3*, 1981.

DeMore, W. B., M. J. Molina, R. T. Watson, D. M. Golden, R. F. Hampson, M. J. Kurylo, C. J. Howard, and A. R. Ravishankara, Chemical kinetics and photochemical data for use in stratospheric modeling: Evaluation number 6, *JPL Publ.*, *83-62*, 1983.

Derwent, R. G., and A. E. G. Eggleton, On the validation of one-dimensional CFC-ozone depletion models, *Nature*, *293*, 387–389, 1981.

de Zafra, R. L., A. Parrish, P. M. Solomon, and J. W. Barrett, A measurement of stratospheric HO_2 by ground-based millimeter wave spectroscopy, *J. Geophys. Res.*, *89*, 1321–1326, 1984.

Evans, W. F. J., J. B. Kerr, D. I. Wardle, J. C. McConnell, B. A. Ridley, and H. I. Schiff, Intercomparison of NO, NO_2, and HNO_3 measurements with photochemical theory, *Atmosphere*, *14*, 189–198, 1976.

Fabian, P., J. A. Pyle, and R. J. Wells, Diurnal variations of minor constituents in the stratosphere modeled as a function of latitude and season, *J. Geophys. Res.*, *87*, 4981–5000, 1982.

Garcia, R. R., and S. Solomon, A numerical model of the zonally averaged dynamical and chemical structure of the middle atmosphere, *J. Geophys. Res.*, *88*, 1379–1400, 1983.

Gille, J. C., and J. M. Russell III, The limb infrared monitor of the stratosphere: Experiment description, performance, and results, *J. Geophys. Res.*, *89*, 5125–5140, 1984.

Gille, J. C., J. M. Russell III, P. L. Bailey, E. E. Remsberg, L. L. Gordley, W. F. J. Evans, H. Fischer, B. W. Gandrud, A. Girard, J. E. Harries, and S. A. Beck, Accuracy and precision of the nitric acid concentration determined by the limb infrared monitor of the stratosphere experiment on Nimbus 7, *J. Geophys. Res.*, *89*, 5179–5190, 1984*a*.

Gille, J. C., J. M. Russell III, P. L. Bailey, L. L. Gordley, E. E. Remsberg, J. H. Lienesch, W. G. Planet, F. B. House, L. V. Lyjak, and S. A. Beck, Validation of temperature retrievals obtained by the limb infrared monitor of the stratosphere (LIMS) experiment on Nimbus 7, *J. Geophys. Res.*, *89*, 5147–5160, 1984*b*.

Guthrie, P. D., C. H. Jackman, J. R. Herman, and C. J. McQuillan, A diabatic circulation experiment in a two-dimensional photochemical model, *J. Geophys. Res.*, *89*, 9589–9602, 1984*a*.

Guthrie, P. D., C. H. Jackman, and A. M. Thompson, Methane and carbon monoxide: Budgets and seasonal behavior in a 2-D model simulation, *Eos Trans. AGU*, *65*, 834, 1984*b*.

Harries, J. E., Ratio of HNO_3 to NO_2 concentrations in daytime stratosphere, *Nature*, *274*, 235, 1978.

Harries, J. E., Stratospheric composition measurements as test of photochemical theory, *J. Atmos. Terr. Phys.*, *44*, 591–597, 1982.

Heaps, W. S., and T. J. McGee, Balloon borne LIDAR measurements of stratospheric hydroxyl radicals, *J. Geophys. Res.*, *88*, 5281–5289, 1983.

Heaps, W. S., and T. J. McGee, Progress in stratospheric hydroxyl measurement by balloon-borne LIDAR, *J. Geophys. Res.*, *90*, 7913–7921, 1985.

Jackman, C. H., J. A. Kaye, and P. D. Guthrie, LIMS HNO_3 data above 5 mbar: Corrections based on simultaneous observations of other species, *J. Geophys. Res.*, *90*, 7923–7930, 1985*a*.

Jackman, C. H., R. S. Stolarski, and J. A. Kaye, Two-dimensional monthly average ozone balance from limb infrared monitor of the stratosphere and stratospheric and mesospheric sounder data, *J. Geophys. Res.*, this issue.

Johnston, H. S., and J. Podolske, Interpretations of stratospheric photochemistry. *Rev. Geophys.*, *16*, 491–519, 1978.

Jones, R. L., Satellite measurements of atmospheric composition: Three years' observations of CH_4 and N_2O, *Adv. Space Res.*, *4*, 121–130, 1984.

Jones, R. L., and J. A. Pyle, Observations of CH_4 and N_2O by the Nimbus 7 SAMS: A comparison with in situ data and two-dimensional numerical model calculations, *J. Geophys. Res.*, *89*, 5263–5279, 1984.

Kaye, J. A., and C. H. Jackman, Concentrations and uncertainties of stratospheric trace species inferred from limb infrared monitor of the stratosphere data, 1, Methodology and application to OH and HO_2, *J. Geophys. Res.*, this issue.

Ko, M. K. W., N. D. Sze, M. Livshits, M. B. McElroy, and J. A. Pyle, The seasonal and latitudinal behavior of trace gases and O_3 simulated by a two-dimensional model of the atmosphere, *J. Atmos. Sci*, *41*, 2381–2408, 1984.

McPeters, R. D., D. F. Heath, and P. K. Bhartia, Average ozone profiles for 1979 from the Nimbus 7 SBUV instrument, *J. Geophys. Res.*, *89*, 5199–5214, 1984.

Mihelcic, D., D. H. Ehhalt, G. F. Kulessa, J. Klomfass, M. Trainer, U. Schmidt, and H. Rohrs, Measurements of free radicals in the atmosphere by matrix isolation and electron paramagnetic resonance, *Pure Appl. Geophys.*, *116*, 530–536, 1978.

Miller, C., D. L. Filkin, A. J. Owens, J. M. Steed, and J. P. Jesson, A two-dimensional model of stratospheric chemistry and transport, *J. Geophys. Res.*, *86*, 12039–12065, 1981.

Mount, G. H., D. W. Rusch, J. M. Zawodny, J. F. Noxon, C. A. Barth, G. J. Rottman, R. J. Thomas, G. E. Thomas, R. W. Sanders, and G. M. Lawrence, Measurements of NO_2 in the earth's stratosphere using a limb scanning visible light spectrometer, *Geophys. Res. Lett.*, *10*, 265–268, 1983.

Mount, G. H., D. W. Rusch, J. F. Noxon, J. M. Zawodny, and C. A. Barth, Measurements of stratospheric NO_2 from the Solar Mesosphere Explorer Satellite, 1, An overview of the results, *J. Geophys. Res.*, *89*, 1327–1340, 1984.

NASA, The stratosphere: Present and future, *NASA Ref. Publ. 1049*, 1979.

National Academy of Sciences, *Halocarbons: Effects on stratospheric ozone*, National Academy Press, Washington, D. C., 1976.

National Academy of Sciences, *Causes and Effects of Changes in Stratospheric Ozone: Update 1983*, National Academy Press, Washington, D. C., 1984.

Pyle, J. A., and A. M. Zavody, The derivation of near-global fields of hydrogen-containing radical concentrations from satellite data sets, *Q. J. R. Meteorol. Soc.*, in press, 1985.

Pyle, J. A., A. M. Zavody, J. E. Harries, and P. H. Moffatt, Derivation of OH concentration from satellite infrared measurements of NO_2 and HNO_3, *Nature*, *305*, 690–692, 1983.

Pyle, J. A., A. M. Zavody, J. E. Harries, and P. H. Moffatt, Derivation of OH concentrations from LIMS measurements, *Adv. Space Res.*, *4*, 117–120, 1984.

Remsberg, E. E., J. M. Russell III, J. C. Gille, L. L. Gordley, P. L. Bailey, W. G. Planet, and J. E. Harries, The validation of Nimbus 7 LIMS measurements of ozone, *J. Geophys. Res.*, *89*, 5161–5178, 1984*a*.

Remsberg, E. E., J. M. Russell III, L. L. Gordley, J. C. Gille, and P. L. Bailey, Implications of the stratospheric water vapor distribution as determined from the Nimbus 7 LIMS experiment, *J. Atmos. Sci.*, *41*, 2934–2945, 1984*b*.

Rodgers, C. D., R. L. Jones, and J. J. Barnett, Retrieval of temperature and composition from Nimbus 7 SAMS measurements, *J. Geophys. Res.*, *89*, 5280–5286, 1984.

Russell, J. M., III, E. E. Remsberg, L. L. Gordley, J. C. Gille, and P. L. Bailey, The variability of stratospheric nitrogen compounds observed by LIMS in the winter of 1978–1979, *Adv. Space Res.*, *2*, 169–172, 1983.

Russell, J. M., III, J. C. Gille, E. E. Remsberg, L. L. Gordley, P. L. Bailey, H. Fischer, A. Girard, S. R. Drayson, W. F. J. Evans, and J. E. Harries, Validation of water vapor results measured by the limb infrared monitor of the stratosphere experiment on Nimbus 7, *J. Geophys. Res.*, *89*, 5115–5124, 1984*a*.

Russell, J. M., III, J. C. Gille, E. E. Remsberg, L. L. Gordley, P. L. Bailey, S. R. Drayson, H. Fischer, A. Girard, J. E. Harries, and W. F. J. Evans, Validation of nitrogen dioxide results measured by the limb infrared monitor of the stratosphere (LIMS) experiment on Nimbus 7, *J. Geophys. Res.*, *89*, 5099–5107, 1984*b*.

Russell, J. M., III, S. Solomon, L. L. Gordley, E. E. Remsberg, and L. Callis, The variability of stratospheric and mesospheric NO_2 in the polar winter night observed by LIMS, *J. Geophys. Res.*, *89*, 7267–7275, 1984*c*.

Russell, J. M., III, The global distribution and variability of stratospheric constituents measured by LIMS, *Adv. Space Res.*, *4*, 107–116, 1984.

Solomon, S., and R. R. Garcia, On the distribution of nitrogen dioxide in the high-latitude stratosphere, *J. Geophys. Res.*, *88*, 5229–5239, 1983.

Stolarski, R. S. Uncertainty and sensitivity studies of stratospheric photochemistry, in *Proceedings of the NATO Advanced Study Institute on Atmospheric Ozone*, edited by A. C. Aikin, pp. 865–876, U.S. Department of Transportation, Federal Aviation Administration, Washington, D. C., 1980.

Thomas, R. J., C. A. Barth, D. W. Rusch, and R. W. Sanders, Solar mesosphere explorer near-infrared spectrometer: Measurements of 1.27-μm radiances and the inference of mesospheric ozone, *J. Geophys. Res.*, *89*, 9569–9580, 1984.

Waters, J. W., J. C. Hardy, R. F. Jarnot, and H. M. Pickett, Chlorine monoxide radical, ozone, and hydrogen peroxide: Stratospheric measurements by microwave limb sounding, *Science*, *214*, 61–64, 1981.

World Meteorological Organization, The stratosphere 1981: Theory and measurements, *Rep. 11*, Global Ozone Res. and Monit. Proj., Geneva, Switzerland, 1982.

C. H. Jackman and J. A. Kaye, Atmospheric Chemistry and Dynamics Branch, Code 616, NASA Goddard Space Flight Center, Greenbelt, MD 20771.

(Received May 1, 1985;
revised September 6, 1985;
accepted September 6, 1985.)